Early Disk-Galaxy Formation from JWST to the Milky Way
Proceedings IAU Symposium No. 377, 2024
F. Tabatabaei, B. Barbuy & Y.-S. Ting, eds.
doi:10.1017/S1743921323001795

Formation of the First Massive Galaxies in Cosmological Simulations and Their Observational Properties

Hidenobu Yajima

Center for Computational Sciences, University of Tsukuba, Ten-nodai, 1-1-1 Tsukuba, Ibaraki 305-8577, Japan. email: yajima@ccs.tsukuba.ac.jp

Abstract. We study the formation of the first massive galaxies and their observational properties for comparisons with JWST or ALMA data by performing cosmological radiative-hydrodynamics simulations. We find that galaxies in overdense regions have high star formation rates larger than ~ 10 $M_\odot$ yr^{-1} at z=10 and their stellar masses reach 10^9 $M_\odot$. The star formation rates of our model galaxies at $z \lesssim 12$ nicely match recent JWST data. In addition, we show that the morphology of galaxies drastically changes with time via major mergers and stellar feedback.

Keywords. stars: Population III, galaxies: evolution, galaxies: formation, galaxies: high-redshift

1. Introduction

Revealing the galaxy formation in the early Universe is a central issue in today's astronomy. In particular, the first-generation galaxies are responsible for ionizing sources of cosmic reionization (Yajima et al. 2009, 2011, 2014). Recent observations by JWST have successfully opened a new window to probe the first galaxies. For example, candidate galaxies at $z \gtrsim 10$ (e.g., Naidu et al. 2022). Donnan et al. (2023) showed 44 new candidate galaxies and developed the UV luminosity functions at the redshifts $z = 8 - 15$. Harikane et al. (2023) found candidate galaxies at $z \sim 17$ with large stellar masses and star formation rates (see also, Naidu et al. 2022). However, the formation of the first galaxies has been poorly understood.

According to the standard theory of structure formation, star formation begins in mini-halos with the halo masses of $\sim 10^6$ $M_\odot$. Thereafter, the first galaxies form via mergers of halos and matter accretion. The first galaxy formation involves complicated processes such as the transition of stellar population from population III to II, the inhomogeneous metal enrichment due to supernovae (e.g., Chiaki & Wise 2019), and UV radiation feedback (e.g., Wise et al. 2012).

Abe et al. (2021) investigated the first galaxy formation with population III stars and indicated that the physical properties of the first galaxies with $M_{\rm h} \sim 10^{8-9}$ $M_\odot$ sensitively depended on the initial mass function of population III stars. They also showed that the UV brightness of the modelled galaxies was fainter than the observable flux levels of JWST. The simulated halo masses in previous works have been limited to $\sim 10^9$ $M_\odot$. Therefore, modeling of more massive bright galaxies is required to compare with observations.

2. Methodology

Here, we study the galaxy formation in overdense regions in which the halo mass exceeds 10^{11} $M_\odot$ at $z \sim 10$. Our simulations allow us to follow the transition from

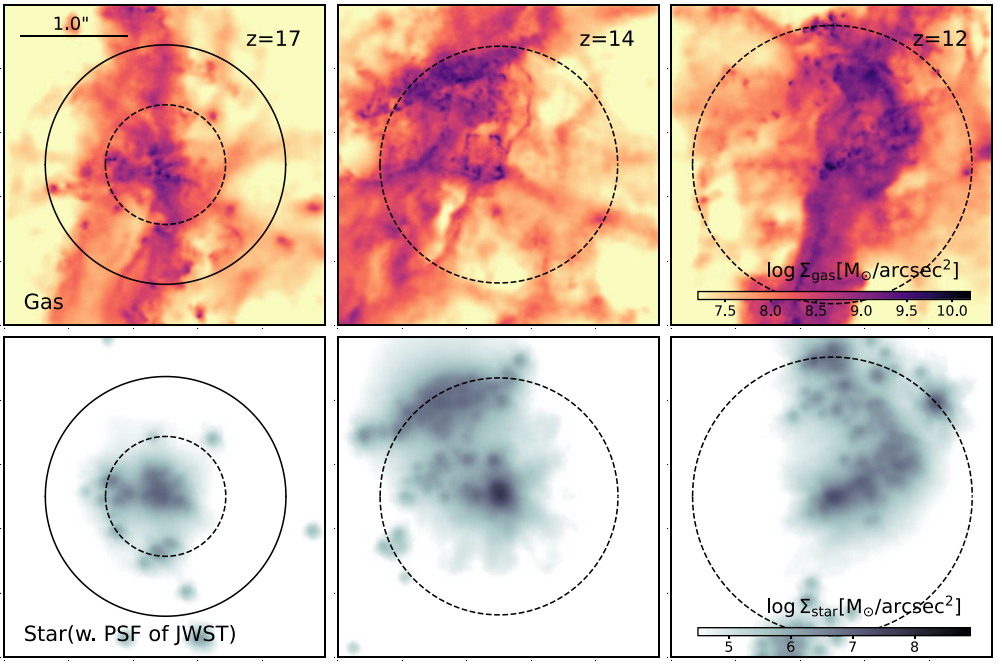

Figure 1. Column density maps of gas and stars in the most massive progenitors at $z = 12, 14$ and 17. The stellar distributions are smoothed with the point spread function of JWST. Solid and dashed circles represent virial radii and half virial radii, respectively. The size of the boxes is 3 arcsec, corresponding to a physical scale of $L = 11.0, 9.8$ and 8.4 kpc at $z = 12, 14$ and 17, respectively.

population III to II stars by resolving mini-haloes. The simulations are part of the simulation project FOREVER22 (Yajima et al. 2022a) that focused 10 overdense regions in the cosmic volume of $(714\ \mathrm{cMpc})^3$. We utilize the GADGET-3 code (Springel 2005) with sub-grid models developed in the OWLS project (Schaye et al. 2010) and the FIBY project (Johnson et al. 2013). Furthermore, we have newly updated the code to handle the photoionization feedback, the radiation pressure on dust, dust growth/destruction, black hole growth, and its feedback (see more, Yajima et al. 2022b).

In this work, we perform two simulations of the first galaxies (First0 and First1 runs). To follow the galaxy formation with high resolutions, we consider zoom-in regions with the volumes of $V \sim (3\ \mathrm{cMpc})^3$ and the mass resolution of an SPH particle $m_{\rm SPH} = 7.9 \times 10^3\ \mathrm{M}_\odot$. The simulations end at $z = 9.5$ when the most massive halo reaches $M_{\rm h} = 5.0 \times 10^{11}\ \mathrm{M}_\odot$. We adopt the cosmological parameters as $\Omega_{\rm M} = 0.3, \Omega_{\rm b} = 0.045, \Omega_\Lambda = 0.7, \sigma_8 = 0.82$ and $h = 0.7$ (Komatsu et al. 2011; Planck Collaboration 2020).

3. Results

Figure 1 shows the column density maps of gas and stars. We make the stellar distributions smoothed with a point spread function of JWST. Along the large-scale filament structure, the gas accretes onto galaxies. The sizes and morphology of stars change with time significantly. At $z = 17$, there are stellar clumps at distances between 0.5 and 1.0 $R_{\rm vir}$, which are likely due to minor mergers. The size of stellar components increases via the baryon accretion and decreases rapidly when major mergers happen (see also, Ono et al. 2022).

Redshift evolutions of halo, stellar masses, and star formation rate (SFR) are shown in Figure 2. The halo masses of the main progenitors are $\sim 10^9\ \mathrm{M}_\odot$ at $z \sim 20$ and reach

https://doi.org/10.1017/S1743921323001795 Published online by Cambridge University Press

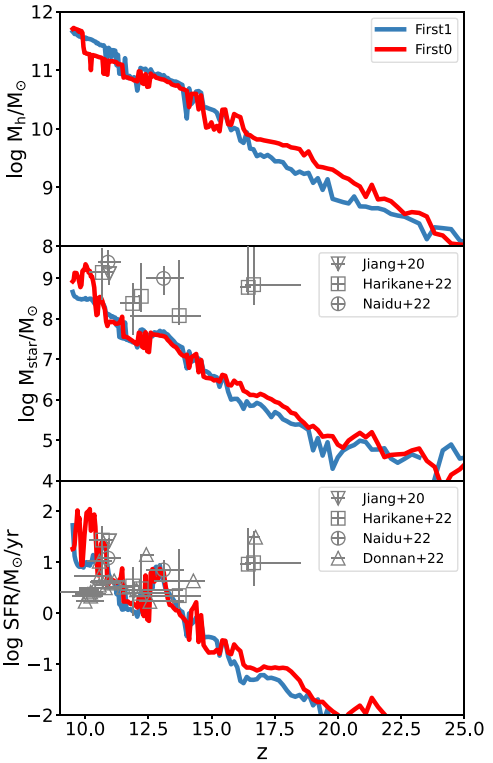

Figure 2. Redshift evolution of the halo, stellar mass, and star formation rate. The red (blue) lines represent the properties of the most massive progenitors in the First0 (First1) runs, respectively. Open symbols show the observations: inverted triangles (Jiang et al. 2021), squares (Harikane et al. 2023), circles (Naidu et al. 2022), and triangles (Donnan et al. 2023).

$\sim 10^{11.5}$ $M_\odot$ at $z \sim 10$. Merger processes induce fluctuations in the halo masses evaluated from the FOF group finder. The abundance of the halo with $10^{11.5}$ $M_\odot$ at $z = 10$ is $dN/dlnM_h \sim 2 \times 10^{-7}$ cMpc^{-3}. Note that, the rarity changes with time even for the most massive progenitors in the same region because of the variety of the halo merger history.

The stellar masses are higher than 10^8 $M_\odot$ at $z \sim 12$ and finally reach $8.4(4.6) \times 10^8$ $M_\odot$ in the First0 (First1) run. These stellar masses match the observed galaxies at $z \lesssim 12$. Note that, however, the stellar masses at $z \sim 17$ are much lower than the observed ones. The observed candidate galaxies $z \sim 17$ indicate high conversion efficiencies from the gas to stars which can be $0.1 - 0.3$ (Inayoshi et al. 2022). Our simulations show that the star formation is efficiently suppressed due to the supernova feedback. The star formation efficiencies (M_{star}/M_{gas}) are $0.1, 2.2 \times 10^{-3}$ and 1.6×10^{-3} at $z = 10, 14$ and 17.

The SFR also increases with the growth of halo mass with large fluctuations. As shown by Yajima et al. (2017), the stellar feedback and the rapid gas accretion induce the cycle of starbursts and quenching. Main progenitor galaxies have $\gtrsim 1$ $M_\odot$ yr^{-1} at $z \lesssim 14$ and show starbursts with SFR $= 109.5$ $M_\odot$ yr^{-1} at $z = 10.2$. Given that the star formation rate is evaluated as $SFR = \epsilon \frac{M_{gas}}{\tau_{dyn}}$ where ϵ is an efficiency parameter and τ_{dyn} is the dynamical time, the starburst at $z \sim 10.2$ corresponds to $\epsilon \sim 0.4$. This value is much larger than typical star-forming galaxies in the local Universe. In the last period of 0.1 Gyr ($z = 9.5 - 11.5$), the halo mass of the main progenitors in the First0 run increases from 7.5×10^{10} $M_\odot$ to 5.0×10^{11} $M_\odot$. We suggest that the rapid growth of halos can induce the starburst. The SFRs of our modeled galaxies at $z \lesssim 14$ agrees well with the

https://doi.org/10.1017/S1743921323001795 Published online by Cambridge University Press

observed ones by JWST (Naidu et al. 2022; Donnan et al. 2023; Harikane et al. 2023) and GN-z11 at $z = 10.957$ (Jiang et al. 2021).

4. Discussion

We have performed cosmological hydrodynamics simulations with feedback processes from UV radiation from massive stars, supernovae, and AGNs. The feedback efficiencies can sensitively depend on environments, numerical resolution, and star formation models (Yajima et al. 2017). In particular, the burst and the quenching of star formation in dwarf galaxies are sensitive to them. Also, the physical properties of the first galaxies are closely related to the initial mass function of population III stars. We will investigate these impacts on the first galaxy formation in future work.

References

Abe, M., Yajima, H., Khochfar, S., Dalla Vecchia, C., Omukai, K. 2021, *MNRAS*, 508, 3226
Chiaki, G., Wise, J. H. 2019, *MNRAS*, 482, 3933
Donnan, C. T., McLeod, D. J., Dunlop, J. S., *et al.* 2023, *MNRAS*, 518, 6011
Inayoshi, K., Harikane, Y., Inoue, A. K., Li, W., Ho, L. C. 2022, *ApJ* (Letters), 938, 10L
Harikane, Y., Ouchi, M., Oguri, M., *et al.* 2023, *ApJS*, 265, 5
Jiang, L., Kashikawa, N., Wang, S., *et. al.* 2021, *Nature Astronomy*, 5, 256
Johnson, J. L., Dalla Vecchia, C., Khochfar, S. 2013, *MNRAS*, 428, 1857
Komatsu, E., Smith, K. M., Dunkley, J., *et al.* 2011, *ApJS*, 192, 18
Naidu, R. P., Oesch, P. A., van Dokkum, P., *et al.* 2022, *ApJ* (Letters), 940, 14L
Ono, Y., Harikane, Y., Ouchi, M., *et al.* submitted to *ApJ*, arXiv:2208.13582
Planck Collaboration, Aghanim, N., Akrami, Y., *et al.* 2020, *A&A*, 641, 6
Schaye, J., Dalla Vecchia, C., Booth, C. M. 2010, *MNRAS*, 402, 1536
Springel, V. 2005, *MNRAS*, 364, 1105
Yajima, H., Umemura, M., Mori, M., Nakamoto, T. 2009, *MNRAS*, 398, 715
Yajima, H., Choi, J. -H., Nagamine, K. 2011, *MNRAS*, 412, 411
Yajima, H., Li, Y., Zhu, Q., Abel, T., Gronwall, C., Ciardullo, R. 2014, *MNRAS*, 440, 776
Yajima, H., Nagamine, K., Zhu, Q., Khochfar, S., Dalla Vecchia, C. 2017, *ApJ*, 846, 30
Yajima, H., Abe, M., Khochfar, S., *et al.* 2022, *MNRAS*, 509, 4037
Yajima, H., Abe, M., Fukushima, H., *et al.* submitted to *MNRAS*, arXiv:2211.12970
Wise, J. H., Turk, M. J., Norman, M. L., Abel, T. 2012, *ApJ*, 745, 50

https://doi.org/10.1017/S1743921323001795 Published online by Cambridge University Press